Antibiotic monensin provides a novel chemotherapy possibility to melanoma

Haoran Xin [1], **Jie Li** [1], **Hao Zhang** [2], **Yuhong Li** [1], **Shuo Zeng** [3], **Zhi Wang** [1], **Zhihui Zhang** [Corresp., 4], **Fang Deng** [Corresp. 1]

[1] Department of Cell Biology, The Third Military Medical University, Chongqing, China
[2] People's Liberation Army of China -32137, Zhangjiakou, Hebei Province, China
[3] Career Education Center, The Third Military Medical University, Chongqing, China
[4] Department of Cardiology, Southwest Hospital, The Third Military Medical University, Chongqing, China

Corresponding Authors: Zhihui Zhang, Fang Deng
Email address: xyzpj@126.com, celldf@tmmu.edu.com

Melanoma is the most lethal cutaneous malignancy that threatens human lives. Poor sensitivity to chemotherapy drugs and the high rate of resistance are the bottlenecks of melanoma treatment. Thus, new chemotherapy drugs are needed. Drug repurposing is a safe, economical and timesaving way to explore new chemotherapy for diseases. Here, we investigated the possibility of repurposing the antibiotic monensin as an anti-melanoma agent. Using three human melanoma celllines and two nomal human cell lines as cell models, we found that monensin is obviously toxic to human melanoma cells while safe to nomal human cells. It effectively inhibits cell proliferation, migration, invasion and cell cycle progression, when promotes apoptosis and differentiation of human melanoma cells in vitro. By establishment of an animal model of transplanted human melanoma in nude mice, we demonstrated that monensin suppressed the growth of xenografts in vivo. Furthermore, we detected that monensin affected multiple cancer-related pathways, including TCF/LEF, Smad and STAT3, and the anti-melanoma mechanism may be inducing terminal differentiation of melanoma.

Antibiotic monensin provides a novel chemotherapy possibility to melanoma

Haoran Xin [1], Jie Li [1], Hao Zhang [2] , Yuhong Li [1], Shuo Zeng[3] , Zhi Wang [1], Zhihui Zhang [4], Fang Deng [1]

[1]Department of Cell Biology, The Third Military Medical University (Army Medical University), Chongqing, China
[2]People's Liberation Army of China -32137, Zhangjiakou, Hebei Province, China
[3]Career Education Center, The Third Military Medical University (Army Medical University), Chongqing, China
[4]Department of Cardiology, Southwest Hospital, The Third Military Medical University (Army Medical University), Chongqing, China

Corresponding Author:
Fang Deng[1]
Gaotanyan street, Shapingba District, Chongqing, 400038, China
Email address: celldf@tmmu.edu.com
Zhihui Zhang[4]
Gaotanyan street, Shapingba District, Chongqing, 400038, China
Email address: xyzpj@126.com

Abstract

Melanoma is the most lethal cutaneous malignancy that threatens human lives. Poor sensitivity to chemotherapy drugs and the high rate of resistance are the bottlenecks of melanoma treatment. Thus, new chemotherapy drugs are needed. Drug repurposing is a safe, economical and timesaving way to explore new chemotherapy for diseases. Here, we investigated the possibility of repurposing the antibiotic monensin as an anti-melanoma agent. Using three human melanoma celllines and two nomal human cell lines as cell models, we found that monensin is obviously toxic to human melanoma cells while safe to nomal human cells. It effectively inhibits cell proliferation, migration, invasion and cell cycle progression, when promotes apoptosis and differentiation of human melanoma cells in vitro. By establishment of an animal model of transplanted human melanoma in nude mice, we demonstrated that monensin suppressed the growth of xenografts in vivo. Furthermore, we detected that monensin affected multiple cancer-related pathways, including TCF/LEF, Smad and STAT3, and the anti-melanoma mechanism may be inducing terminal differentiation of melanoma.

Introduction

Melanoma is a highly malignant tumor, with mortality as high as 80%(Cummins et al. 2006). As the early symptoms of melanoma are not obvious, most patients have been diagnosed in the middle and late stages. Melanoma is not sensitive to radiotherapy, and the treatment is mainly dependent on chemotherapy. However, poor sensitivity to chemotherapy drugs and easy resistance are the bottleneck of melanoma treatment. The front-line clinical anticancer agents used for melanoma are mainly in five categories, including alkylating agents, anti-CTLA4 monoclonal antibodies, BRAFV600E inhibitors, C-KIT inhibitors and PD-1 inhibitors. Representative drugs include Dacarbazine, Ipilimumab, Vemurafenib, Imatinib and Nivolumab. The natural resistance rate of melanoma in order is 87.5%, 88%, 70% (white) ~85% (yellow), 98.8% (white) ~89.2% (yellow), and 74%(Guo et al. 2012; Wu et al. 2014). Therefore, there is an urgent need to develop effective new drugs. However, An invention of a new drug usually faces a long research period, large risk of fail and biosafty problems.

In recent years, drug reposition has attracted increasing attention. Drug reposition means exploring the new pharmacological effects of drugs whose biosafety and pharmacokinetics are known and extending thier applicationsproperties in therapies for other diseases. The advantages of drug-reposition are their short development period, high biosafety, low cost and known side effects. Drug reposition has become a new hot spot in the field of cancer treatment.

Monensin is secreted by the bacteria *Streptomyces cinnamonensis*(Pressman 1968), and it is used to kill coccidia parasites and improve the feed conversion rate of ruminant animals. It has been reported that monensin shows a good therapeutic effect in a variety of tumors, including ovarian cancer, colon cancer, myeloma and lymphoma(Deng et al. 2015; Park et al. 2003a; Park et al. 2003b; Park et al. 2002). However, it remains unclear whether monensin has anticancer effects on human melanoma cells.

To explore the possibility of anti-melanoma effect of monensin , in vitro, we examined the effects of monensin on proliferation, cell cycle, migration and apoptosis of several human melanoma cell lines. In vivo, the effects of monensin on tumor growth was investigated by xenograft animal model. We found that monensin efficiently suppressed human melanoma at a biosafe dose, and then we discussed the foundation mechenisms of the effect.

Materials & Methods

Cell culture and drug

Human melanoma cells A375, Mel-624, Mel-888, Human embryonic kidney cells HEK-293 and Human bladder epithelium immortalized cells SV-HUC-1 were all purchased from the American Type Culture Collection (ATCC, Manassas, VA, USA). The cells were cultured in complete DMEM containing 10% fetal bovine serum (FBS, Invitrogen, Carlsbad, CA, USA), 100 units of penicillin and 100 μg of streptomycin, at 37˚C in 5% CO2. Drug monensin sodium salt was purchased from Solarbio (Beijing, China) and dissolved in ethanol. All the procedures were in strict accordance with the Institutional Review Board of The Third Military Medical University.

Crystal violet cell viability assay

A375, Mel-624 and Mel-888 cells were treated with varied concentrations of monensin or ethanol control, respectively. At 24 h, 48 h and 72 h after treatment, cells were washed with PBS and fixed with 0.4% paraformaldehyde at room temperature for 20 min. Then cells stained with 0.5% crystal violet (Beyotime, Shanghai, China) at room temperature for 20 min. The cells were washed with tape water and air dried before imaging. For quantification, the cells were incubated with 100% acetic acid at room temperature for 20 min with shaking. The absorbance was set at 570 nm.

Viable cell counting assay

A375, Mel-624 and Mel-888 cells were treated with monensin at the varied concentrations or ethanol control. At 24 h, 48 h and 72 h, cells were collected by trypsin dissociation, and stained with Trypan blue (Beyotime, Shanghai, China). Unstained viable cells and total cells were counted under a bright field microscope (Nikon, Tokyo, Japan).

Cell cycle analysis

A375, Mel-624 and Mel-888 cells were seeded in 6-well plates and treated with varied concentrations of monensin or ethanol control. At 4 h, 8 h, 12 h after treatment, cells were collected, fixed and stained with the propidium iodide (Beyotime, Shanghai, China) for 5 min. Then the cells were subjected to flow cytometry analysis using the Flow Cytometer (BD Biosciences, San Jose, CA, USA). The flow cytometry data were analyzed with the FlowJo v10.0 software.

CCK-8 cytotoxicity assay

Cytotoxicity was assessed by using cell counting kit-8 (CCK-8; Dojindo, Tokyo, Japan). A375, Mel-624, Mel-888, HEK-293 and SV-HUC-1 cells seeded in 96-well plates were treated with varied concentrations of monensin or ethanol control for 24 h, 48 h and 72 h. 10 μL CCK-8 reagent was added to each well, followed by an incubation at 37℃ for 60 min and reading at 450 nm using the microplate reader (Bio-RAD, California, USA).

Wound healing assay

A375, Mel-624 and Mel-888 cells were seeded in 24-well cell culture plates. When grew at 90% confluency, the cells were scratched with a sterile micro-pipette tip and treated with varied concentrations of monensin or ethanol control. The images were taken under a bright field microscopy (Nikon, Tokyo, Japan) at 0 h, 24 h, 48 h and 72 h after cell scratch.

Transwell cell invasion assay

2×10^4 A375, Mel-624 and Mel-888 cells were seeded in the upper chamber of a 24-well transwell device (8-μm, Merck Millipore, Burlington, MA, USA), coated with matrigel (Corning), in 200 μl serum-free medium, and 600 μL of medium containing 10% FBS was added to the bottom chamber. Then cells were treated with varied concentrations of monensin or

ethanol control in the upper chamber. At 24 h, 36 h and 48 h after treatment, cells migrating into the lower surface of the chambers were fixed with 0.4% paraformaldehyde for 20 min and stained with 0.5% crystal violet for 20 min. Then, the cells on the upper surface of the filter and matrigel were removed using a cotton swab. Five fields were imaged per transwell insert, and the number of cells was counted.

Hoechst 33258 staining

A375, Mel-624 and Mel-888 cells were seed in a 6-well plate with cover glasses respectively and treated with varied concentrations of monensin or ethanol control. At 8 h, 12 h and 16 h after treatment, cells were fixed and stained with Hoechst Staining Kit (Beyotime, Shanghai, China). Apoptotic cells were examined under a fluorescence microscope. The average number of apoptotic cells was calculated in at least ten random fields at 200x magnification for each assay.

Annexin V-FITC flow cytometry assay

A375 , Mel-624 and Mel-888 cells were seeded in 6-well plates respectively and treated with varied concentrations of monensin or ethanol control. At 4 h, 8 h and 12 h after treatment, cells were dissociated with trypsinization, washed with PBS, and resuspended in Annexin V Binding Buffer at a density of 10^6 cells/ml. Then the cells were stained with Annexin V-FITC (BD Pharmingen, San Jose, CA) for half an hour, followed by counterstaining with propidium iodide for 15 min at room temperature. After wash, the cells were subjected to flow cytometry analysis using the BD FACSCalibur-HTS. Data were analyzed by using the FlowJo v10.0 software. Each assay was done in triplicate.

Xenograft of human melanoma cells

The use and care of animals were approved by the Laboratory Animal Welfare and Ethics Committee Of the Third Military Medical University (Approval Number SYXK (Chongqing) 20170002). A375 stably labeled with firefly luciferase (A375-FLuc) was constructed with piggyBac system(Chen et al. 2015; Wang et al. 2014; Wen et al. 2014). A375-Luc cells were collected and resuspended at 10^7 cells/ml. 100ul cells were subcutaneously injected into the dorsal back skin of athymic nude mice (4-week-old, male, 10^6 cells per injection, and 2 sites per mouse). The mice were divided into two groups (n = 5 per group). At three days post injection, the animals were treated with various doses of monensin (25 mg/kg or 50 mg/kg body weight) or vehicle control (ethanol) by oral administration once a day. Tumor growth was monitored by whole body bioluminescence imaging using Xenogen IVIS 200 Imaging System at days 4, 7 and 10 after injection. The mice were sacrificed at 10 days and subcutaneous tumor masses were harvested for examination.

Luciferase reporter assay

The Gaussia luciferase (GLuc) reporter assay was carried out as described(Gao et al. 2013; Li et al. 2013; Zhang et al. 2015). The tyrosinase reporter and 12 cancer-relate signaling pathway

reporters were homemade and previously described(Gao et al. 2013), including NFAT, HIF-1,TCF/LEF, Elk1/SRF, AP1, NFκB, Smad, STAT3, RBP-Jκ, CREB, Myc/Max, GR reporters. A constitutively active reporter pG2Luc was used as a control. Experimentally, A375 cells were seeded in 25 cm^2 culture flasks and transfected with 1.0 μg per flask of the 12 reporter plasmids using Lipofectamine (Invitrogen, Carlsbad, CA). At 16 h post transfection, cells were replated in 12-well plates and treated with various concentrations of monensin or ethanol control. At 24 h, 48 h or 72 h post treatment, culture media were taken and subjected to Gaussia luciferase assays using the BioLux Gaussia Luciferase Assay Kit (New England Biolabs). Each assay condition was done in triplicate. Luciferase activity was normalized by total cellular protein concentrations among the samples.

Sphere formation assay

A375, Mel-624 and Mel-888 cells were seeded in complete medium and placed at 10^7 cells per 6-well Ultra Low Cluster plates (Corning) with varied concentrations of monensin or ethanol control. At 24 h, 48 h and 72 h post treatment, images were recorded at 100x magnification and the maximum diameter of cell mass were measured.

Colony formation assay

A375, Mel-624 and Mel-888 cells were diluted in complete medium and seeded at 1000 cells per 6-well. Cells were treated with monensin at the varied concentrations and ethanol control for 24 h, then replaced the medium and continuted to culture for 6 days in DMEM supplemented with 10% FBS. After 6 days, the colonies were fixed with 0.4% paraformaldehyde for 20 min and stained with 0.5% crystal violet for 15min. The plates were washed and visible colonies were counted and colony forming efficiency (CFE) was calculated. The colonies that were less than 2 mm in diameter or faintly stained were excluded. CFE was defined as the number of colonies divided by the number of cells seeded and expressed as percentage.

Statistical analysis

Data were expressed as mean ± SD. Statistical significance of experimental results was determined by Student's T-test to compare the differences among two groups. For multiple group comparison, one-way ANOVA analysis of variance was performed followed by multiple comparison tests. The statistical analysis was performed using GraphPad Prism 6 (GraphPad Software, La Jolla, USA). P value less than 0.05 was considered as a significant difference.

Results

Monensin is obviously toxic to human melanoma cells

To test whether monensin can decrease the livability of human melanomasubconfluent A375, Mel-624 and Mel-888 cells were grown in increasing concentrations of monensin. Crystal violet staining results showed that cell proliferation of A375, Mel-624 and Mel-888 cells was significantly inhibited in the monensin-treated groups compared to the control group (ethanol

control group), especially in A375 cells (Figs. 1A and 1B). We also conducted Trypan blue-stained after exponentially growing A375, Mel-624 and Mel-888 cells were treated with varying concentrations of monensin (0 μM to 0.4 μM). The number of viable cells decreased significantly when the concentration of monensin was increased in the three cell lines at all examined time points, especially at 72 h (Fig. 1C). We also performed cell cycle analysis by using flow cytometry of monensin-treated A375, Mel-624 and Mel-888 cells. The number of cells arrested in G1 phase was significantly increased in monensin-treated cells, whereas the number of cells in S/G2/M phase was significantly decreased in monensin-treated melanoma cells, compared to the controls (P value of A375 = 0.002, P value of Mel-624 = 0.008, P value of Mel-888 = 0.0002) (Figs. 1D and 1E). These results suggest that monensin inhibits melanoma cell proliferation, and the inhibition effect was dose-dependent.

Monensin is non-cytotoxic to common human cells at the same dose

We have already know that 0 μM to 0.4 μM monensin was cytotxic to melanoma cells, if we want to use this dose to treat melanoma, side effect should be concerned. So we tested whether monensin is cytotoxic to common human cells at the same doses. Subconfluent human embryonic kidney cells HEK-293 and human bladder epithelium immortalized cells SV-HUC-1 were grown in increasing concentrations of monensin (0 μM to 0.4 μM). Microscopy images of HEK-293 cells and SV-HUC-1 cells showed no significant cell number decrease or morphology changes in the monensin-treated group compared to the control groups (Fig. 2B). CCK-8 cytotoxicity assay also showed that monensin was non-cytotoxic to HEK-293 cells and SV-HUC-1 cells at the indicated concentrations (IC50 cannot be obtained, Fig. 2C). However, statistical analysis of CCK-8 cytotoxicity assay of three melanoma cells showed that monensin inhibited cell activity and was significantly cytotoxic to A375 (IC50 = 0.16 μM), Mel-624 (IC50 = 0.71 μM) and Mel-888 (IC50 = 0.12 μM) (Fig. 2A). Taken together, our results demonstrate that monensin is significantly cytotoxic to melanoma cells but non-cytotoxic to common human cells at the same dose.

Monensin effectively inhibits cell migration and invasion in human melanoma cells

Migration and invasion are important aspects of cancer cellbiology,to test whether monensin can inhibit the cell migration and invasion of human melanoma cells, we performed wound healing and transwell cell invasion assays. Phase-contrast microscopy images and statistical analysis revealed that A375, Mel-624 and Mel-888 cells migrated and closed the wound more slowly in the monensin-treated groups than in the control groups (Figs. 3A and 3B). At 72 h post-treatment, the width of the wound gap, relative to the starting width, was closed 45% and 30% for A375 cells at 0.1 μM and 0.4 μM, respectively, 30% and 29% for Mel-624 cells at 0.1 μM and 0.4 μM, respectively, and 40% and 36% for Mel-888 cells at 0.1 μM and 0.4 μM, respectively. Further, transwell cell invasion assay results showed that melanoma cells treated with monensin (0.1 μM and 0.4 μM) had weaker invasion ability, and this effect was dose-

dependent (Figs. 3C and 3D). These results suggest that monensin effectively inhibits cell migration and invasion in human melanoma cells.

Monensin induces apoptosis of human melanoma cells

Apoptosis may be closely related to the cytotoxic effect of monensin, therefore, we examined cell apoptosis after A375, Mel-624 and Mel-888 cells were treated with 0.4 μM monensin. Hoechst 33258 staining results revealed that the percentage of apoptotic cells was significantly increased in monensin-treated A375, Mel-624 and Mel-888 cells (Figs. 4A and 4B) at 24 h after drug treatment, compared to the control groups (green arrows, live cells; yellow arrows, apoptotic cells). We also checked cell apoptosis by flow cytometry (Fig. 4C). Statistical analysis revealed the proportion of Annexin V+/PI- early apoptotic cells and Annexin V+/ PI+ late apoptotic cells were both increased in the monensin-treated A375 (early 1.9%, late 1%), Mel-624 (early 1.4%, late 0.6%) and Mel-888 (early 1.6%, late 0.6%) cells compared to the control group A375 (early 0.7%, late 0.3%), Mel-624 (early 0.7%, late 0.4%) and Mel-888 (early 0.5%, late 0.2%) cells（Fig. 4D). Together, these results suggest that monensin can induce apoptosis in the human melanoma cell lines A375, Mel-624 and Mel-888.

Monsensin effectively inhibits tumor growth in a xenograft model of human melanoma cells

In view of the obvious inhibitory effect of monensin on melanoma observed at the cell culture level, we are full of expectations about whether it can inhibit the growth of melanoma in vivo. Firefly luciferase-tagged A375 cells were subcutaneously injected into the dorsal back skin of athymic nude mice. At three days post-injection, the animals were treated with various doses of monensin (25 mg/kg or 50 mg/kg body weight) or vehicle control (ethanol) by oral administration once a day. Ten days after injection, the xenografts were collected. Tumor growth was examined using xenogen bioluminescence imaging 4, 7 and 10 days after cell injection (Fig. 5A). Quantitative analysis of the xenogen imaging data revealed that the xenografts that were treated with monensin showed significantly lower luciferase activity compared to that of the control groups (Fig. 5B). The xenografts that were treated with monensin formed significantly smaller tumors in weight compared to the control groups (Fig. 5C). These studies confirmed that monensin can effectively suppress melanoma growth.

Monensin has effects on multiple cancer-related signaling pathways, and the mechanism may be inducing terminal differentiation of melanoma

To test how monensin effects human melanoma cells, we used the Gaussia luciferase reporter gene system. When the Gaussia luciferase reporters for the 12 pathways and a constitutively active reporter pG2Luc were transfected into A375 cells and treated with 0 μM, 0.4 μM or 0.8 μM monensin for 48 h, it was found that Gaussia luciferase activities for the NFAT, TCF/LEF, Smad, STAT3 and Myc/Max reporters were significantly increased compared to the control groups. A slight but apparent up-regulation of HIF-1, AP1 and GR reporter activity was also

noted (Fig. 6A). The results of the Gluc-reporter assay suggested that monensin may target differentiation-related signaling pathways. Interestingly, we observed that melanin granules increased in monensin-treated groups under a phase-contrast microscope (Fig. 6B). Further, we tested the expression of tyrosinase, and the results revealed that the tyrosinase expression of A375, Mel-624 and Mel-888 cells was significantly increased in monensin-treated groups compared to the control groups (Fig. 6C). The increase in melanin granules is a mark of terminal differentiation in melanoma. Pluripotency is the opposite of terminal differentiation, and we also tested cell pluripotency maintenance after monensin treatment. The microscope images and statistical analysis of sphere formation assay revealed that the sphere formation ability of A375, Mel-624 and Mel-888 cells was significantly decreased in monensin-treated group, compared to the control groups (P value of A375 = 0.0146, P value of Mel-624 = 0.0004, P value of Mel-888 = 0.0178) (Figs. 6D and 6E). At the same time, we also tested the pluripotency of the three melanoma cell lines by colony formation assay. The results revealed that monensin can significantly inhibit the proliferation of melanoma, and this effect was shown at a low concentration of just 0.025 μM. Sphere formation assays and colony formation assays both suggest that monensin can inhibit the pluripotency of melanoma. Taken together, these results strongly suggest that monensin may mainly target differentiation-related signaling pathways, and the mechanism may be inducing terminal differentiation of melanoma.

Discussion

Monensin may be repurposed as an effective anticancer agent for human melanoma.

The status quo of chemotherapy has revealed that poor sensitivity to chemotherapy drugs and easy resistance are the bottlenecks of melanoma treatment. Thus, there is a critical need to develop more effective and novel therapies to treat melanoma. Our results have demonstrated that monensin has efficient antitumor activity and effectively inhibits cell proliferation, migration, invasion and cell cycle progression, and it promotes apoptosis and differentiation of human melanoma cells.

Monensin is FDA-approved for veterinary use (beef cattle, dairy cattle, and chickens), and it is used to kill coccidia parasites and improves the feed conversion rate of ruminant animals. The in vivo dose of monensin we used in this study for its anticancer activity was much less than the maximum dose (200 mg/herd/day) for the prevention and control of coccidiosis(Deng et al. 2015). Our results have demonstrated that monensin is non-cytotoxic to common human cells HEK-293 and SV-HUC-1 at the same dose we used to treat melanoma cells (0 μM to 0.4 μM). These results reveal that monensin has a favorable safety profile and acts effectively at low micromolar concentrations. Moreover, the in vitro dose used in this study was also much less than other tumor cells. The IC50 of monensin to melanoma cells A375, Mel-624 and Mel-888 was 0.16 μM, 0.70 μM and 0.12 μM, respectively. This is a lower dose needed to achieve its anticancer activity in other tumors (IC50 is 2.5 μM in colon cancer cells and 1 μM in myeloma cells) (Park et al. 2003a; Park et al. 2003b). This finding suggests that melanoma has a higher sensitivity to monensin. Although there is still no definite clinical evidence that can prove

monensin is lowly toxic to humans, some studies in mammals indicate that the level of residues of monensin in edible animal tissues remains too low to adversely affect the health of consumers(Dorne et al. 2013).

Monensin may exert its anticancer activity by targeting differentiation-related signaling pathways.

We demonstrated that monensin has an anticancer effect on human melanoma, and further investigation of the detailed mechanism is needed. In earlier studies, monensin induced apoptosis-associated changes in Bax, caspase-3, and caspase-8(Park et al. 2002), elevated intracellular oxidative stress(Ketola et al. 2010) in several human cancer cells, or exerted effects on the intracellular trafficking and processing of endocytosis(Nishimura et al. 2015). However, few reports suggest that monensin may target cancer cells through differentiation-related signaling pathways.

In our study, we found that monensin up-regulates the reporter activities for the TCF/LEF, Smad, STAT3 and Myc/Max pathways. Interestingly, TCF/LEF(Larue et al. 2003), Smad(Moustakas 2008) and STAT3(Hirano et al. 2000) are all associated with cell differentiation. At the same time, we found that the expression of tyrosinase and melanin granules, marks of terminal differentiation in melanoma stem cells, were both significantly increased; however, the pluripotency maintenance ability of melanoma was decreased. Thus, our results strongly suggest that monensin may exert its strong antiproliferative activity by promoting differentiation-related signaling pathways, such as TCF/LEF, Smad, and STAT3. These results provide a new idea that we can induce differentiation of melanoma cells to treat human melanoma, similar to what we do in acute promyelocytic leukemia(Wang & Chen 2008).

Conclusions

In summary, we investigated the potential of repurposing monensin as an anti-cancer agent for human melanoma. Monensin was shown to target multiple cancer-related signaling pathways and the anti-melanoma mechanism of monensin may be inducing terminal differentiation of melanoma. Future studies should be directed towards testing monensin's anti-cancer efficacy in preclinical and clinical studies.

Acknowledgements

We would like to thank Professor Yun Wang and Professor Yizhan Xing (Department of Cell Biology, Third Military Medical University) for their advice on cell cycle analysis and xenograft assay.

References

Chen X, Cui J, Yan Z, Zhang H, Chen X, Wang N, Shah P, Deng F, Zhao C, Geng N, Li M, Denduluri SK, Haydon RC, Luu HH, Reid RR, and He TC. 2015. Sustained high level

transgene expression in mammalian cells mediated by the optimized piggyBac transposon system. Genes Dis 2:96-105. 10.1016/j.gendis.2014.12.001

Cummins DL, Cummins JM, Pantle H, Silverman MA, Leonard AL, and Chanmugam A. 2006. Cutaneous malignant melanoma. Mayo Clin Proc 81:500-507. 10.4065/81.4.500

Deng Y, Zhang J, Wang Z, Yan Z, Qiao M, Ye J, Wei Q, Wang J, Wang X, Zhao L, Lu S, Tang S, Mohammed MK, Liu H, Fan J, Zhang F, Zou Y, Liao J, Qi H, Haydon RC, Luu HH, He TC, and Tang L. 2015. Antibiotic monensin synergizes with EGFR inhibitors and oxaliplatin to suppress the proliferation of human ovarian cancer cells. Sci Rep 5:17523. 10.1038/srep17523

Dorne JL, Fernandez-Cruz ML, Bertelsen U, Renshaw DW, Peltonen K, Anadon A, Feil A, Sanders P, Wester P, and Fink-Gremmels J. 2013. Risk assessment of coccidostatics during feed cross-contamination: animal and human health aspects. Toxicol Appl Pharmacol 270:196-208. 10.1016/j.taap.2010.12.014

Gao JL, Lv GY, He BC, Zhang BQ, Zhang H, Wang N, Wang CZ, Du W, Yuan CS, and He TC. 2013. Ginseng saponin metabolite 20(S)-protopanaxadiol inhibits tumor growth by targeting multiple cancer signaling pathways. Oncol Rep 30:292-298. 10.3892/or.2013.2438

Guo H, Yang K, Deng F, Xing Y, Li Y, Lian X, and Yang T. 2012. Wnt3a inhibits proliferation but promotes melanogenesis of melan-a cells. Int J Mol Med 30:636-642. 10.3892/ijmm.2012.1028

Hirano T, Ishihara K, and Hibi M. 2000. Roles of STAT3 in mediating the cell growth, differentiation and survival signals relayed through the IL-6 family of cytokine receptors. Oncogene 19:2548-2556. 10.1038/sj.onc.1203551

Ketola K, Vainio P, Fey V, Kallioniemi O, and Iljin K. 2010. Monensin is a potent inducer of oxidative stress and inhibitor of androgen signaling leading to apoptosis in prostate cancer cells. Mol Cancer Ther 9:3175-3185. 10.1158/1535-7163.MCT-10-0368

Larue L, Kumasaka M, and Goding CR. 2003. Beta-catenin in the melanocyte lineage. Pigment Cell Res 16:312-317.

Li M, Chen Y, Bi Y, Jiang W, Luo Q, He Y, Su Y, Liu X, Cui J, Zhang W, Li R, Kong Y, Zhang J, Wang J, Zhang H, Shui W, Wu N, Zhu J, Tian J, Yi QJ, Luu HH, Haydon RC, He TC, and Zhu GH. 2013. Establishment and characterization of the reversibly immortalized mouse fetal heart progenitors. Int J Med Sci 10:1035-1046. 10.7150/ijms.6639

Moustakas A. 2008. TGF-beta targets PAX3 to control melanocyte differentiation. Dev Cell 15:797-799. 10.1016/j.devcel.2008.11.009

Nishimura Y, Takiguchi S, Ito S, and Itoh K. 2015. EGFstimulated AKT activation is mediated by EGFR recycling via an early endocytic pathway in a gefitinibresistant human lung cancer cell line. Int J Oncol 46:1721-1729. 10.3892/ijo.2015.2871

Park WH, Kim ES, Jung CW, Kim BK, and Lee YY. 2003a. Monensin-mediated growth inhibition of SNU-C1 colon cancer cells via cell cycle arrest and apoptosis. Int J Oncol 22:377-382.

Park WH, Kim ES, Kim BK, and Lee YY. 2003b. Monensin-mediated growth inhibition in NCI-H929 myeloma cells via cell cycle arrest and apoptosis. Int J Oncol 23:197-204.

Park WH, Lee MS, Park K, Kim ES, Kim BK, and Lee YY. 2002. Monensin-mediated growth inhibition in acute myelogenous leukemia cells via cell cycle arrest and apoptosis. Int J Cancer 101:235-242. 10.1002/ijc.10592

403 Pressman BC. 1968. Ionophorous antibiotics as models for biological transport. Fed Proc
404 27:1283-1288.
405 Wang N, Zhang W, Cui J, Zhang H, Chen X, Li R, Wu N, Chen X, Wen S, Zhang J, Yin L,
406 Deng F, Liao Z, Zhang Z, Zhang Q, Yan Z, Liu W, Ye J, Deng Y, Wang Z, Qiao M, Luu
407 HH, Haydon RC, Shi LL, Liang H, and He TC. 2014. The piggyBac transposon-mediated
408 expression of SV40 T antigen efficiently immortalizes mouse embryonic fibroblasts
409 (MEFs). PLoS One 9:e97316. 10.1371/journal.pone.0097316
410 Wang ZY, and Chen Z. 2008. Acute promyelocytic leukemia: from highly fatal to highly
411 curable. Blood 111:2505-2515. 10.1182/blood-2007-07-102798
412 Wen S, Zhang H, Li Y, Wang N, Zhang W, Yang K, Wu N, Chen X, Deng F, Liao Z, Zhang J,
413 Zhang Q, Yan Z, Liu W, Zhang Z, Ye J, Deng Y, Zhou G, Luu HH, Haydon RC, Shi LL,
414 He TC, and Wei G. 2014. Characterization of constitutive promoters for piggyBac
415 transposon-mediated stable transgene expression in mesenchymal stem cells (MSCs).
416 PLoS One 9:e94397. 10.1371/journal.pone.0094397
417 Wu N, Zhang H, Deng F, Li R, Zhang W, Chen X, Wen S, Wang N, Zhang J, Yin L, Liao Z,
418 Zhang Z, Zhang Q, Yan Z, Liu W, Wu D, Ye J, Deng Y, Yang K, Luu HH, Haydon RC,
419 and He TC. 2014. Overexpression of Ad5 precursor terminal protein accelerates
420 recombinant adenovirus packaging and amplification in HEK-293 packaging cells. Gene
421 Ther 21:629-637. 10.1038/gt.2014.40
422 Zhang H, Wang J, Deng F, Huang E, Yan Z, Wang Z, Deng Y, Zhang Q, Zhang Z, Ye J, Qiao
423 M, Li R, Wang J, Wei Q, Zhou G, Luu HH, Haydon RC, He TC, and Deng F. 2015.
424 Canonical Wnt signaling acts synergistically on BMP9-induced osteo/odontoblastic
425 differentiation of stem cells of dental apical papilla (SCAPs). Biomaterials 39:145-154.
426 10.1016/j.biomaterials.2014.11.007
427

Figure 1

Monensin inhibits the proliferation of human melanoma cells

(A) Crystal violet staining revealed that there were fewer live cells in melanoma cells A375, Mel-624 and Mel-888 treated with monensin at the indicated concentrations for 72 h, compared to the control groups. (B) Quantitative analysis of the Crystal violet-stained cells revealed that there were significantly fewer live cells in melanoma cells treated with monensin at the indicated concentrations for 72 h, compared to the control groups. (C) Quantitative analysis of Trypan blue-stained cells showed that there were fewer viable cells in melanoma cells A375, Mel-624 and Mel-888 treated with monensin at the indicated concentrations for 24 h, 48 h and 72 h, compared to the control groups. (D) Cell cycle analysis showed that there were fewer cells in S/G2/M phase in monensin-treated groups, compared to the control groups. (E) Statistical analysis of cell cycle study showed that there were significantly fewer cells in S/G2/M phase in monensin-treated groups at 12 h after treatment, compared to the control groups. *$p < 0.05$; **$p < 0.01$; ***$p < 0.001$; ****$p < 0.0001$.

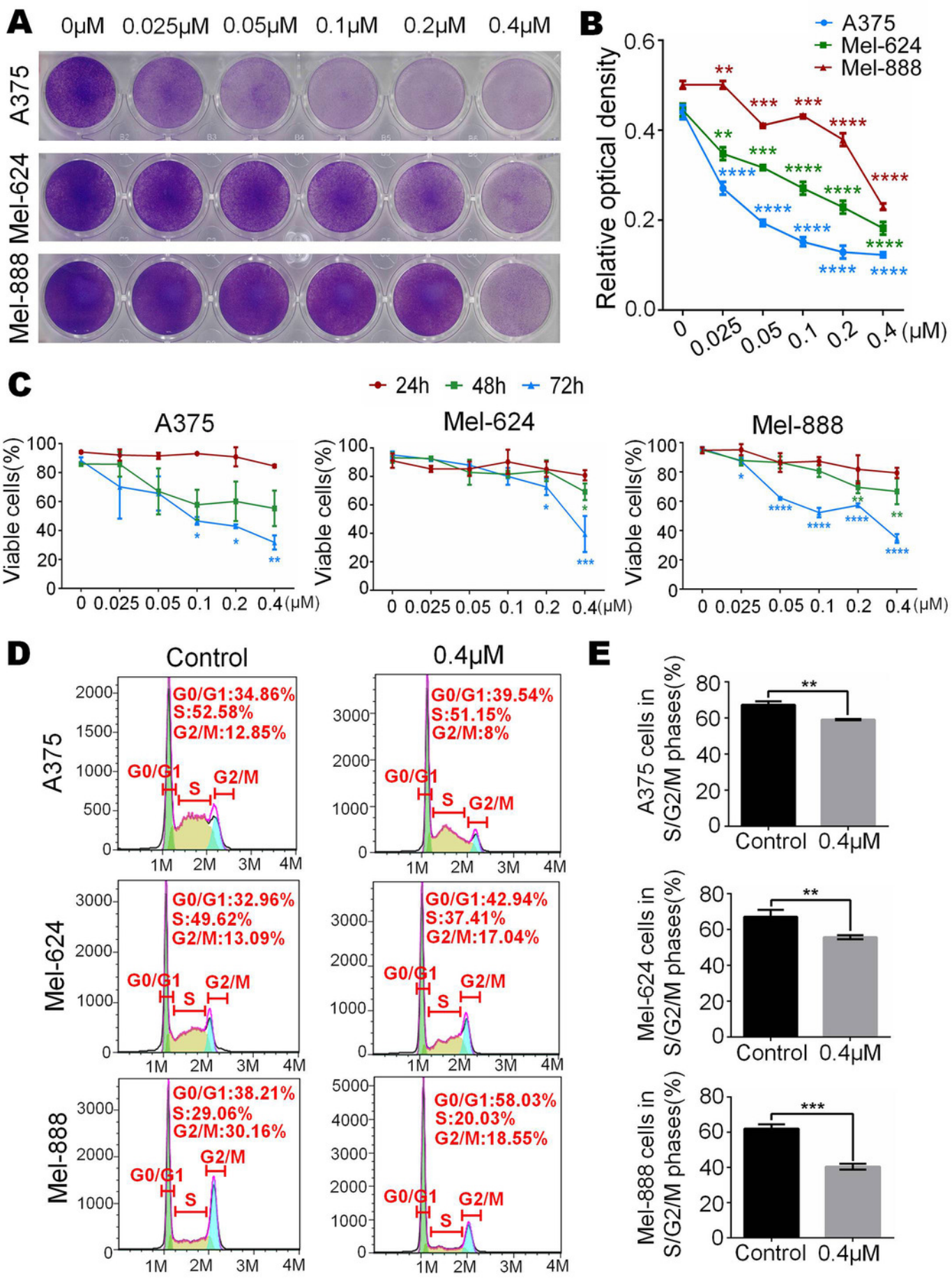
A
0μM 0.025μM 0.05μM 0.1μM 0.2μM 0.4μM
A375
Mel-624
Mel-888
B
A375
Mel-624
Mel-888
Relative optical density
0.6
0.4
0.2
0.0
0 0.025 0.05 0.1 0.2 0.4 (μM)
C
24h 48h 72h
A375
Mel-624
Mel-888
Viable cells(%)
100
80
60
40
20
0
0 0.025 0.05 0.1 0.2 0.4(μM)
D
Control
0.4μM
A375
Mel-624
Mel-888
G0/G1:34.86%
S:52.58%
G2/M:12.85%
G0/G1:39.54%
S:51.15%
G2/M:8%
G0/G1:32.96%
S:49.62%
G2/M:13.09%
G0/G1:42.94%
S:37.41%
G2/M:17.04%
G0/G1:38.21%
S:29.06%
G2/M:30.16%
G0/G1:58.03%
S:20.03%
G2/M:18.55%
G0/G1
S
G2/M
1M 2M 3M 4M
E
A375 cells in S/G2/M phases(%)
Mel-624 cells in S/G2/M phases(%)
Mel-888 cells in S/G2/M phases(%)
Control 0.4μM

Figure 2

Monensin is non-cytotoxic to common human cells at the same dose

(A) CCK-8 cytotoxicity assay revealed fewer live cells in melanoma cells A375, Mel-624 and Mel-888 treated with monensin at the indicated concentrations for 72h, compared to the control groups. Absorbance, 450 nm. Each assay was done in triplicate. (B) Microscopy images revealed no decrease of HEK-293 and SV-HUC-1 treated with 0.4μM monensin for 72h, compared to the control groups. (C) CCK-8 cytotoxicity assay revealed no significant decrease of HEK-293 and SV-HUC-1 treated with monensin at the indicated concentrations for 72h, compared to the control groups. Absorbance, 450 nm. *p < 0.05; **p < 0.01; ***p < 0.001; ****p < 0.0001.

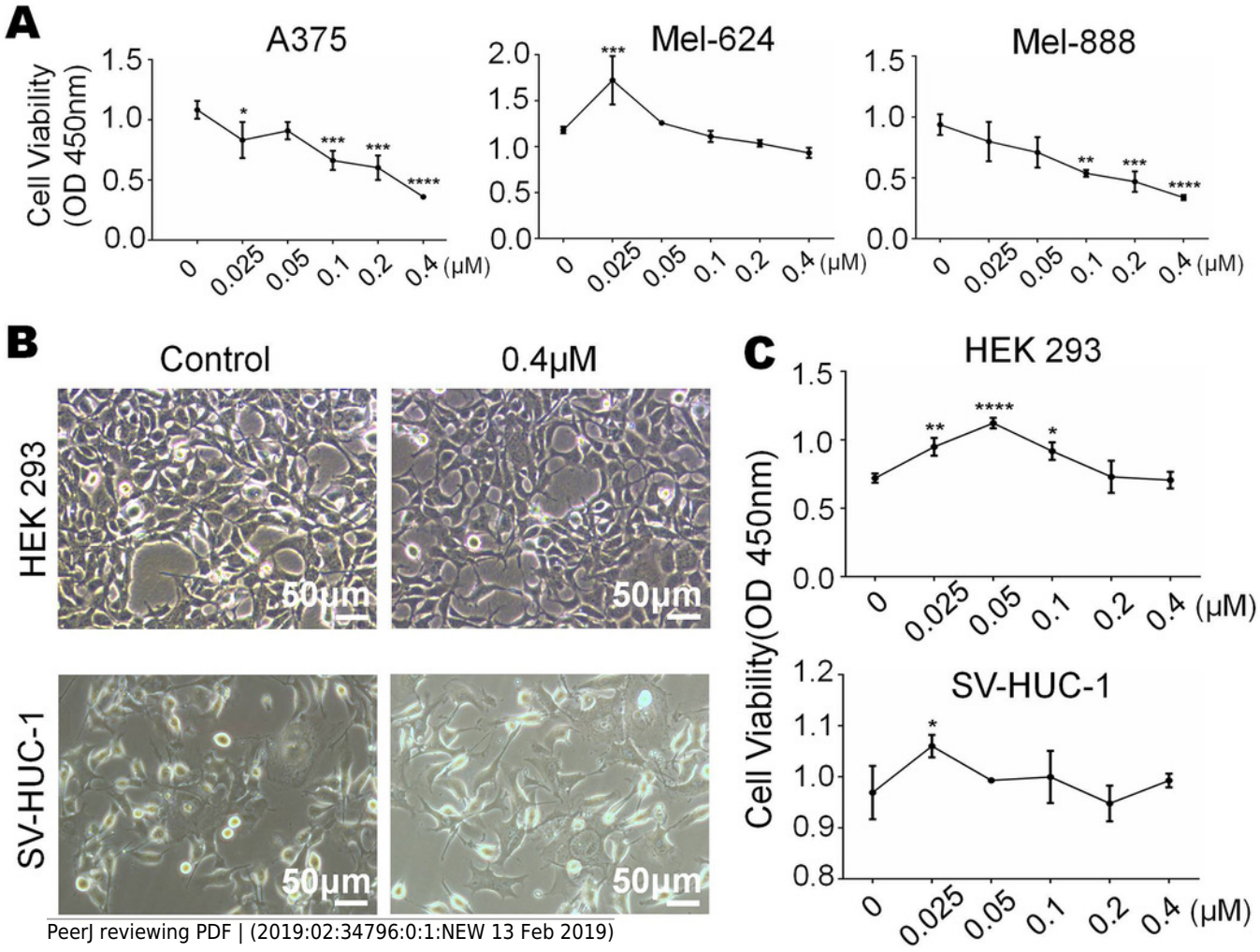

Figure 3

Monensin effectively inhibits cell migration and invasion in human melanoma cells

(A) Wound healing assay showed that the scratch gaps of A375, Mel-624 and Mel-888 were wider in the monensin-treated group s, compared to the control groups. (B) Statistical analysis of wound healing assay showed that the wound closure rates of A375, Mel-624 and Mel-888 were significantly decreased in the monensin-treated groups, compared to the control groups. The wound gaps were recorded at 72 h after treatment with 0.1 μM and 0.4 μM monensin. (C) Transwell cell invasion assay showed that there were fewer cells of A375, Mel-624 and Mel-888 crossing the matrigel in the monensin-treated groups, compared to the control groups. (D) Statistical analysis of transwell cell invasion assay showed that there were fewer cells of A375, Mel-624 and Mel-888 crossing the matrigel in the monensin-treated groups, compared to the control groups. The invaded cells were recorded at 48 h after treatment with 0.1 μM and 0.4 μM monensin. **$p < 0.01$; ***$p < 0.001$; ****$p < 0.0001$.

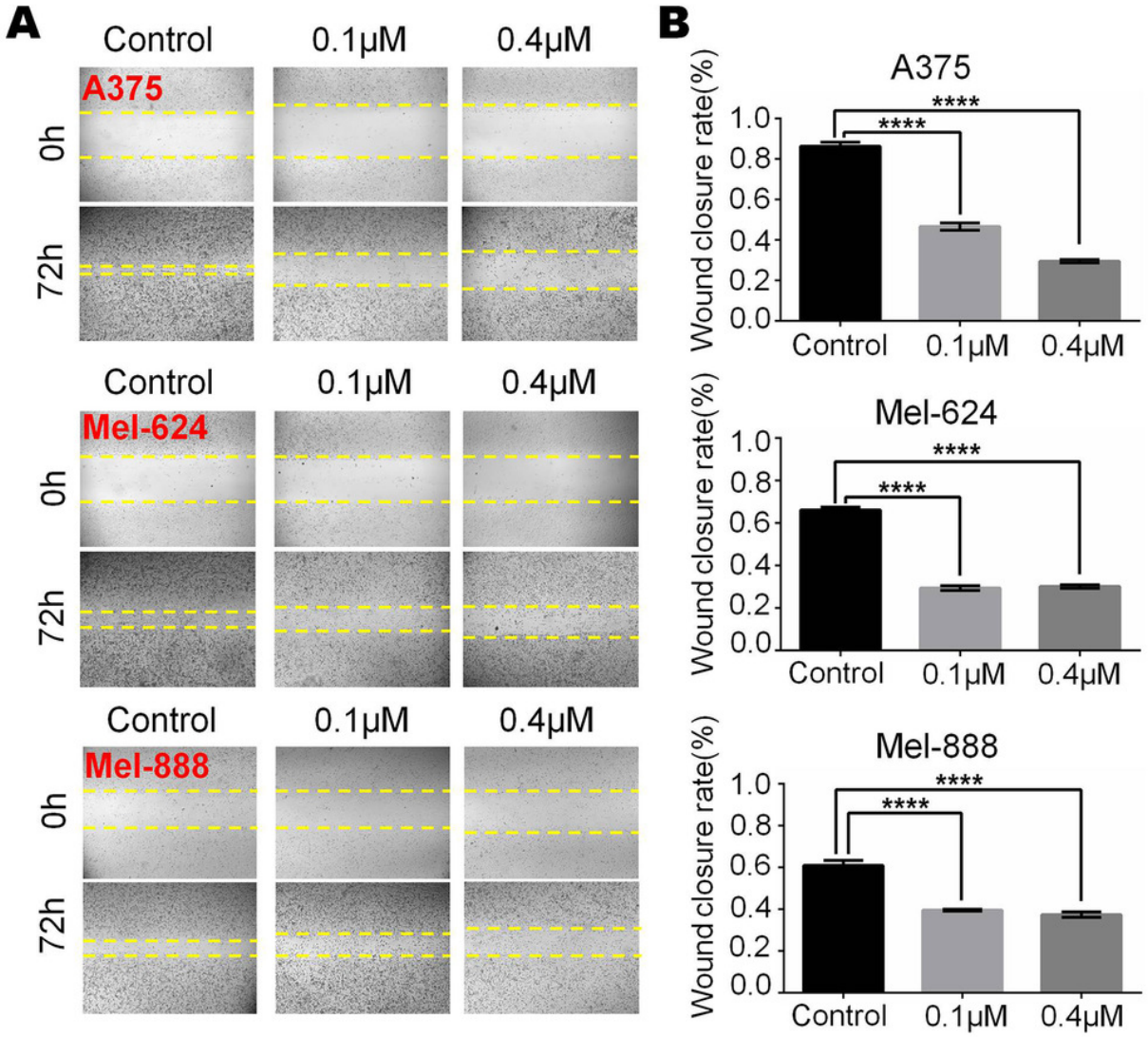
A
Control
0.1μM
0.4μM
A375
0h
72h
Mel-624
Mel-888
B
A375
Mel-624
Mel-888
Wound closure rate(%)
1.0
0.8
0.6
0.4
0.2
0.0
****
Control
0.1μM
0.4μM

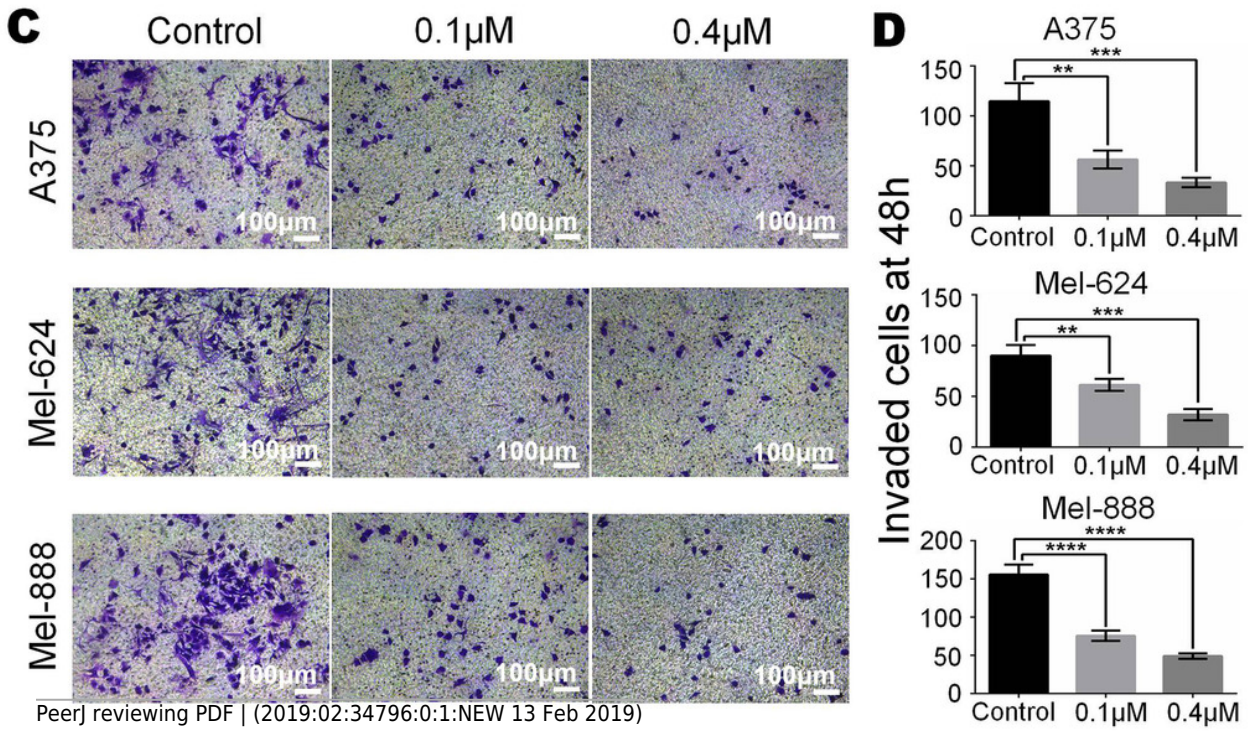
C
Control
0.1μM
0.4μM
A375
Mel-624
Mel-888
100μm
D
A375
Mel-624
Mel-888
Invaded cells at 48h
***
**
****
150
100
50
200
0
Control
0.1μM
0.4μM

Figure 4

Monensin induces apoptosis of human melanoma cells

(A) Hoechst 33258 staining revealed that there were significant more apoptotic cells in monensin-treated groups with 0.4 μM at 16 h post treatment, compared to the control groups. Green arrows, live cells; Yellow arrows, apoptotic cells. (B) Statistical analysis of 16 h revealed that there were significant more late apoptotic cells in monensin-treated group, compared to the control groups. (C) Annexin-V apoptosis assay. A375, Mel-624 and Mel-888 cells were treated with 0.4 μM monensin, respectively. At 12 h post treatment, cells were collected and stained with Annexin V-FITC and propidium iodide, and were subjected to flow cytometry. Average percentages of apoptotic cells were calculated. (D) Statistical analysis revealed that there were more early and late apoptotic cells in monensin-treated groups, compared to the control groups. Each assay was done in triplicate. *p< 0.05; **p< 0.01; ***p< 0.001; ****p< 0.0001; ns = no significant difference.

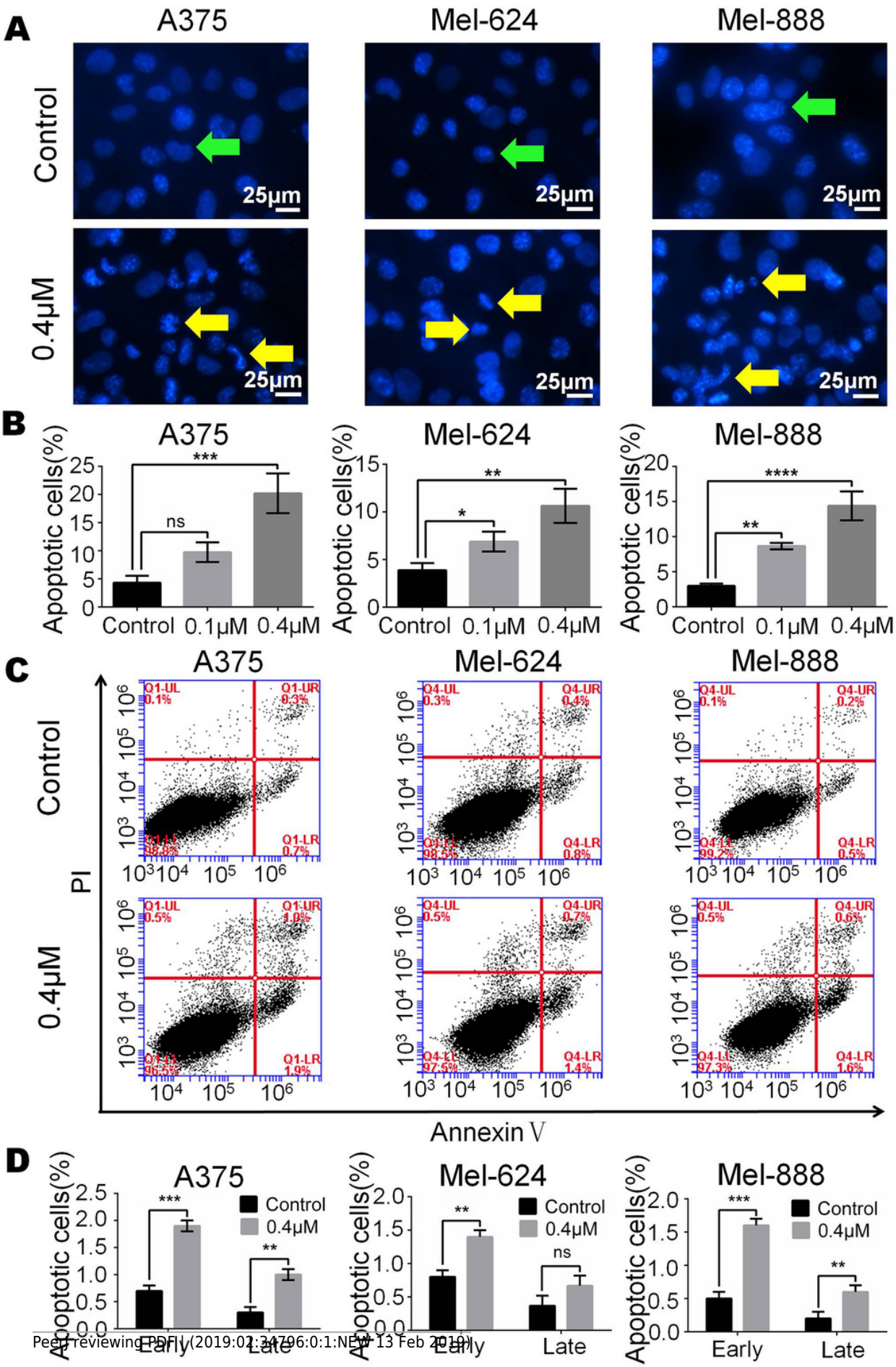
A
A375
Mel-624
Mel-888
Control
0.4μM
25μm
B
A375
Mel-624
Mel-888
Apoptotic cells(%)
Control
0.1μM
0.4μM
ns
C
Control
0.4μM
PI
Annexin V
Q1-UL 0.1%
Q1-UR 0.3%
Q1-LL 98.8%
Q1-LR 0.7%
Q4-UL 0.3%
Q4-UR 0.4%
Q4-LL 98.5%
Q4-LR 0.8%
Q4-UL 0.1%
Q4-UR 0.2%
Q4-LL 99.2%
Q4-LR 0.5%
Q1-UL 0.5%
Q1-UR 1.0%
Q1-LL 96.5%
Q1-LR 1.9%
Q4-UL 0.5%
Q4-UR 0.7%
Q4-LL 97.5%
Q4-LR 1.4%
Q4-UL 0.5%
Q4-UR 0.6%
Q4-LL 97.3%
Q4-LR 1.6%
D
A375
Mel-624
Mel-888
Apoptotic cells(%)
Control
0.4μM
Early
Late
ns

Figure 5

Monensin effectively inhibits tumor growth in vivo

(A) Xenogen bioluminescence imaging of xenograft tumor growth. Firefly luciferase-labeled A375 cells were injected into athymic nude mice subcutaneously. The animals were treated with 0mg/kg, 25mg/kg and 50mg/kg monensin by oral administration once a day. The mice were imaged at 4, 7 and 10 days after cell injection. Representative images at day 7 are shown. (B) The average signal for each group at different time points were calculated using the Xenogen Living Image analysis software. (C) The average tumor weight for each group. *p< 0.05; **p< 0.01; ns = no significant difference.

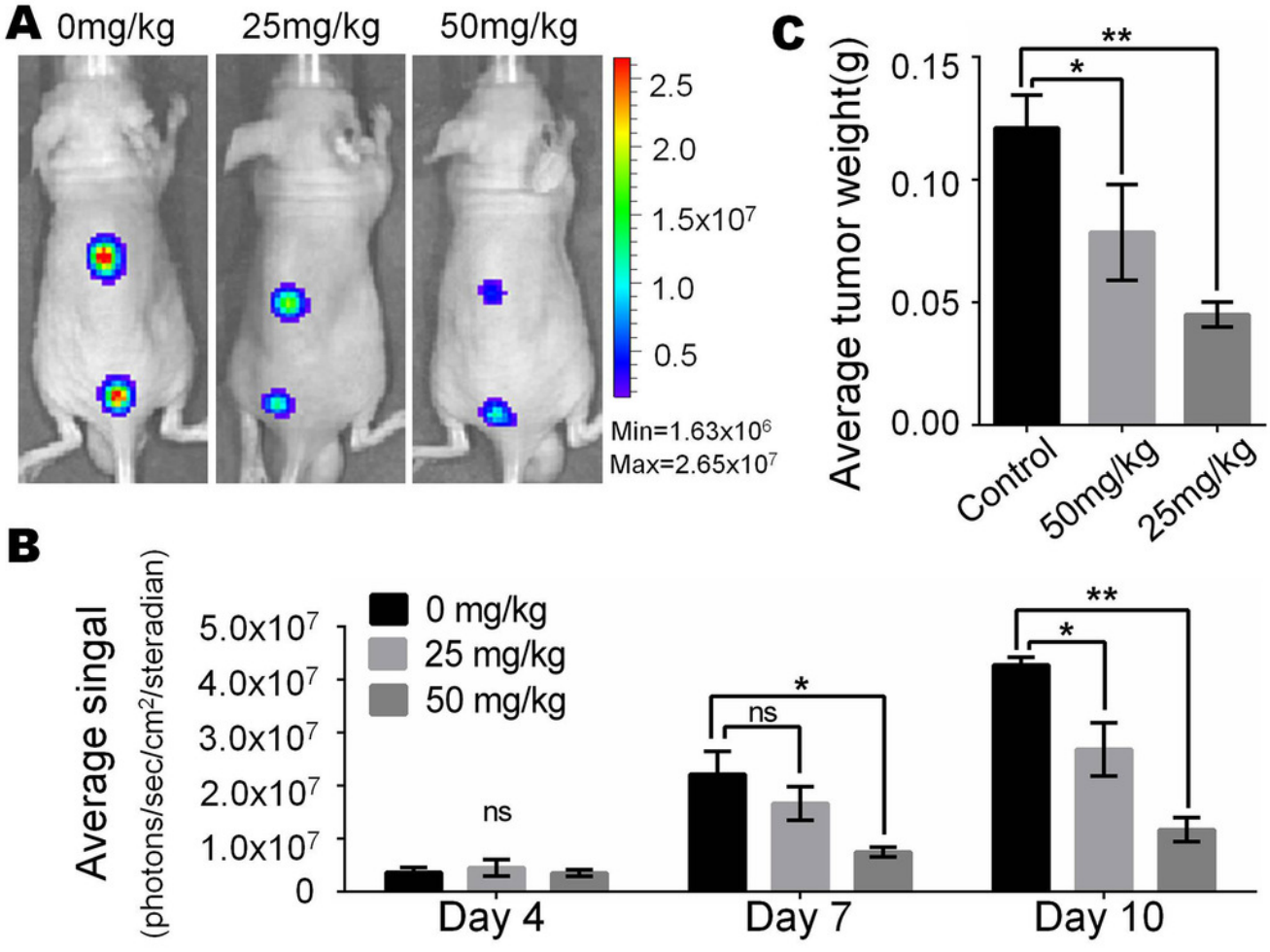

Figure 6

Monensin has effects on multiple cancer-related signaling pathways and the mechanism may be inducing terminal differentiation of melanoma

(A) Quantitative analysis of GLuc reporters of 12 cancer-associated pathway revealed monensin can up-regulate the reporter activities of the 8 cancer-associated pathways. (B) Phase-contrast microscopy images of melanoma cells A375, Mel-624 and Mel-888 revealed melaningranules were increased in monensin-treated groups, compared to the control groups. Yellow arrows, melaningranules. (C) Quantitative analysis of GLuc reporters of tyrosinase showed tyrosinase expression of A375, Mel-624 and Mel-888 cells was increased with the increasing concentrations of monensin after treatment for 72 h . Absorbance, 490 nm. (D) Sphere formation assay reveal ed sphere formation ability of A375, Mel-624 and Mel-888 cells was decreased in monensin-treated groups, compared to the control groups. Representative images at 48 h are shown. (E) Statistical analysis of sphere formation assay at 48 h showed that the sphere diameters are significantly decreased in monensin-treated groups, compared to the control groups. (F) Colony formation assay revealed the total number of colonies was fewer with the increasing concentrations of monensin after treatment for 6 days. Representative images are shown. (G) Quantitative analysis of colony formation assay showed colony forming effciency was significantly decreased in monensin-treated groups, compared to the control groups. *p< 0.05; **p< 0.01; ***p< 0.001; ****p< 0.0001; ns = no significant difference.

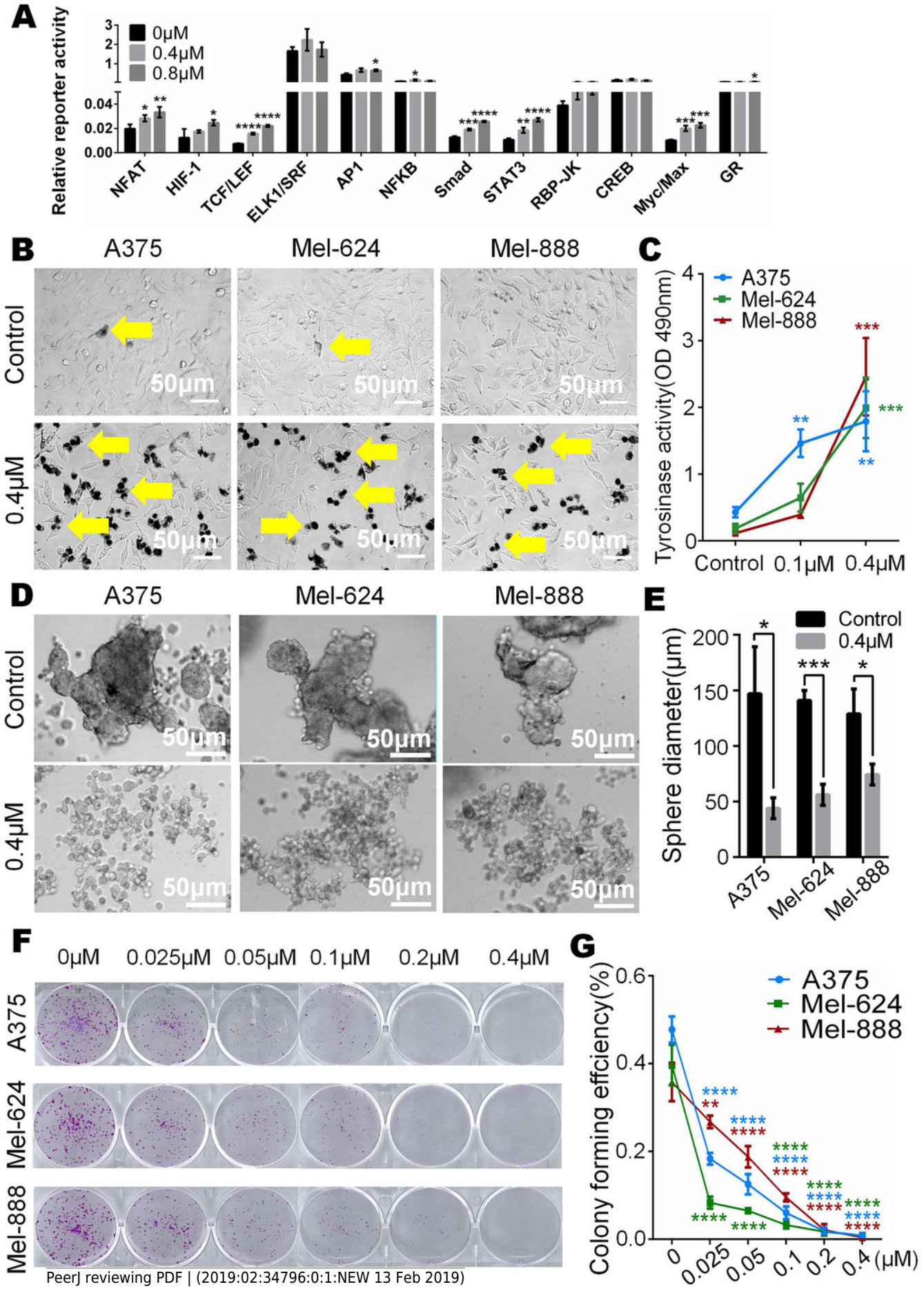
A
Relative reporter activity
0μM
0.4μM
0.8μM
NFAT
HIF-1
TCF/LEF
ELK1/SRF
AP1
NFKB
Smad
STAT3
RBP-JK
CREB
Myc/Max
GR
B
A375
Mel-624
Mel-888
Control
0.4μM
50μm
C
Tyrosinase activity(OD 490nm)
Control
0.1μM
0.4μM
D
E
Sphere diameter(μm)
F
0μM
0.025μM
0.05μM
0.1μM
0.2μM
0.4μM
G
Colony forming effciency(%)
(μM)